J. Phys. Chem. A **2008,** *112,* 1627−1632

Anion−π and π−π Cooperative Interactions Regulating the Self-Assembly of Nitrate−Triazine−Triazine Complexes

Maurizio Zaccheddu,[†] Claudia Filippi,*,[†] and Francesco Buda*,[‡]

Instituut-Lorentz, Leiden University, P.O. Box 9506, 2300 RA Leiden, The Netherlands, and Leiden Institute of Chemistry, Leiden University, P.O. Box 9502, 2300 RA Leiden, The Netherlands

Received: November 27, 2007

We theoretically investigate the cooperative enhancement of the interactions between anions and electron-deficient aromatics by $\pi-\pi$ stacking, focusing on the recent crystallographic observation of anion−$\pi-\pi$ interactions in a synthesized coordination compound based on 1,3,5-triazine moieties. Using a combination of state-of-the-art dispersion-corrected density functional and quantum Monte Carlo calculations, we rationalize the unusual structural features observed in this nitrate−triazine−triazine complex. We show that the triazine rings are staggered and bent and slip with respect to each other with the nitrate bound off-center in a T-like configuration. Our results indicate that this $\pi-\pi$ stacking is not simply enforced by the coordination of the triazines within the particular crystal structure but is regulated by cooperative anion−π and $\pi-\pi$ interactions. In the nitrate−triazine−triazine complex, this cooperative effect amounts to 6% of the total binding energy. Ways to further increase this energetic enhancement in the design of anion−host architectures are discussed.

1. Introduction

The design of selective receptors of anionic species is a very active area of research within supramolecular chemistry due to the potential applications to catalysis, separation processes, and biomolecular systems.[1] Common neutral receptors bind the anion by hydrogen bonding or coordinate the anion at the Lewis acidic center of an organometallic ligand. As compared to cationic hosts, neutral receptors avoid the presence of competing negative counterions and are characterized by higher selectivity due to the directionality of the interactions. In recent years, the alternative route of anion complexation by neutral hosts via anion−π interactions has received considerable interest. The favorable binding interactions between an anionic species and an electron-deficient π-electron compound has been demonstrated in several theoretical studies[2−18] and experimental evidence of these attractive interactions is now cumulating from both X-ray structures[19−27] and solution data.[28,29]

Aromatic systems which have been investigated as potential anion−host candidates are either substituted benzene or electron-poor heteroaromatics such as triazines. Even though π-systems are expected to interact repulsively with anions, the presence of electron-withdrawing substituting atoms in the aromatic compounds modulates the reactivity inverting their natural electron-donor character. Hexafluorobenzene is the extreme example with a permanent quadrupole moment of similar magnitude as benzene but opposite sign, leading to attractive electrostatic interactions with electron-donor species.[30] In general, the interactions between the anion and the π-system are predominantly of electrostatic and polarization nature, but dispersion forces and charge transfer[7,8,16] also contribute to the stability of these complexes.

Recently, experimental evidence of anion−$\pi-\pi$ interactions has emerged from crystallographic studies[20−23] on synthesized coordination compounds based on the electron-deficient 1,3,5-triazine moieties, suggesting the possibility to enhance anion−π binding by $\pi-\pi$ stacking. Particularly intriguing are the structural features of the nitrate−triazine−triazine complex of ref 23, as the two aromatic rings are staggered and not perfectly faced, and the nitrate ion is not parallel to the closest ring. The unusual asymmetrical configuration of the closely stacked triazines could be induced by the particular coordination within the compound, or governed by a subtle interplay between anion−π and $\pi-\pi$ interactions.[15,18] In the original paper, the compound was also investigated theoretically but, due to the poor description of dispersive interactions by the standard density functional theory approach employed, no conclusions could be drawn on the stabilization effect of $\pi-\pi$ interactions on the whole complex.

In the present theoretical study, we investigate and rationalize the structural features of this anion−$\pi-\pi$ complex, and quantitatively address the issue of cooperativity of anion−π and $\pi-\pi$ interactions using a combination of dispersion-corrected density functional theory (DFT) and quantum Monte Carlo (QMC) calculations. The calculated structure is remarkably close to the one observed experimentally even though the anion−$\pi-\pi$ complex was not additionally coordinated as in the crystal structure. Therefore, the unusual stacking is an intrinsic feature which stabilizes the anion−π binding, indicating that the principle of anion−$\pi-\pi$ cooperativity is regulating the self-assembly in this coordination compound. Energetically, the cooperative effect of anion−π and $\pi-\pi$ interactions in the triazine−triazine−nitrate complex is not negligible but amounts to roughly 6% of the total binding energy.

We want to emphasize that the theoretical investigation of anion−$\pi-\pi$ interactions is particularly demanding. In anion−π systems, correlation significantly contributes to the interaction energy[7,8] and must therefore be accurately treated. In the presence of aromatic stacking, the need to also address $\pi-\pi$ interactions further complicates matters. Finally, even though most previous studies of anion−π systems within the MP2

---

* To whom correspondence should be addressed. E-mail: filippi@lorentz.leidenuniv.nl (C.F.) and f.buda@chem.leidenuniv.nl (F.B.).

[†] Instituut-Lorentz.

[‡] Leiden Institute of Chemistry.

10.1021/jp711225x CCC: $40.75

approach were limited to highly symmetrical configurations, it is important to be able to explore lower-symmetry complexes for a realistic representation of the anion−π−π systems observed experimentally. Therefore, we choose here to employ the efficient DFT approach in combination with the recently proposed dispersion-corrected atom-centered pseudopotentials (DCACPs),[31,32] which we validate against accurate highly correlated quantum Monte Carlo calculations. The DFT-DCACP method is found to reliably predict equilibrium structures as well as the relative stability of different complexes and is therefore a very promising tool for the investigation of even larger anion−π systems.

2. Computational Approaches

We briefly review below the two theoretical methods employed in this work, that is, the recently developed semiempirical DFT scheme augmented with dispersion-corrected atom-centered potentials (DCACPs) and the quantum Monte Carlo (QMC) approach. We also give all relevant computational details.

2.1. Semiempirical Dispersion-Corrected DFT. A simple semiempirical approach has been recently proposed to correct the deficiency of approximate density functionals in describing London dispersion forces.[31,32] The nonlocal electron-nucleus pseudopotentials used in the Kohn−Sham DFT scheme are augmented with DCACPs whose parameters are fitted against references data obtained in ab initio highly correlated approaches. By construction, these potentials do not affect valence electronic properties but appear to significantly improve the description within DFT of weakly bound systems at no additional computational cost.[33,34]

Although the original DCACPs were calibrated against MP2 reference properties, we use here the latest library of potentials constructed from more accurate coupled-cluster singles and doubles with a perturbative treatment of the triples [CCSD(T)] and configuration interaction data.[35] We employ the generalized gradient approximation (GGA) functional of Becke, Lee, Yang, and Parr (BLYP)[36] and the corresponding DCACPs nonlocal potentials given in the Troullier−Martins[37] form. We use the DCACPs for all the atomic species except for F where we use the original Troullier−Martins BLYP pseudopotential as the corresponding DCACP is not yet available. We expect that the absence of dispersion corrections for F is not important in the complexes studied in section 3.3 as the F−F interaction is dominated by electrostatic repulsion. All the DFT calculations are performed using the plane-wave basis set program CPMD 3.11.1[38] with a plane-wave cutoff of 80 Ry. We employ the isolated system module in CPMD, which allows studying an isolated molecule or complex within periodic boundary conditions. The Poisson equations are solved with the Hockney method.[39] We use a box size of 15 × 15 × 15 Å^3, which is sufficiently large for all the complexes considered in this work. All the geometry optimizations are performed without imposing any symmetry constraints and with a threshold for the residual force of 0.0005 au. The binding energies of complexes are computed by subtracting the energies of the optimized fragments from the total energy of the complex. We note that all computed binding energies do not include zero point energy corrections.

2.2. Quantum Monte Carlo Methods. QMC methods[40,41] offer an efficient alternative to conventional highly correlated ab initio methods as they can be applied to sufficiently large systems and still provide an accurate description of both dynamical and static electronic correlation. The key ingredient that determines the quality of a QMC calculation is the many-body trial wave function which, in the present work, is chosen of the Jastrow−Slater type with the particular form,

$$\Psi = D^{\uparrow}D^{\downarrow}\prod_{A,i,j}\mathcal{J}(r_{ij},r_{iA},r_{jA}) \tag{1}$$

where $D^{\uparrow}$ and $D^{\downarrow}$ are Slater determinants of single-particle orbitals for the up- and down-spin electrons, respectively, and the orbitals are represented using atomic Gaussian basis. The Jastrow correlation factor $\mathcal{J}$ depends on the distance r_{ij} between electrons i and j, and on the distance r_{iA} and r_{jA} of electrons i and j from nucleus A. The Jastrow factor is here expressed as the exponential of the sum of three fifth-order polynomials of electron−nuclear, of electron−electron, and of pure three-body mixed electron−electron and electron−nucleus distances, respectively.[42] Different Jastrow factors are used to describe the correlation with different atom types.

In variational Monte Carlo (VMC), the square of the wave function is sampled using the Metropolis algorithm and the expectation value of the Hamiltonian on the wave function is computed by statistically averaging over a large number of electronic configurations sampled from Ψ^2. The wave function is then used in diffusion Monte Carlo (DMC), which produces the best energy within the fixed-node approximation, *i.e.*, the lowest-energy state with the same zeros (nodes) as the trial wave function Ψ. All QMC results presented below are from DMC calculations.

All QMC calculations are performed with the program package CHAMP.[43] We employ scalar-relativistic energy-consistent Hartree−Fock pseudopotentials[44] for all the elements, and the hydrogen potential is softened by removing the Coulomb divergence. To represent the orbitals in the determinantal component, we employ the Gaussian basis sets[44] constructed for these pseudopotentials and augment them with diffuse functions. All calculations are performed with the cc-pVDZ basis augmented with two additional diffuse s and p functions with exponents 0.04690 and 0.04041 for carbon, 0.06124 and 0.05611 for nitrogen, 0.07896 and 0.06856 for oxygen, and 0.06080 and 0.04660 for chlorine.[45] Only in the computation of the binding energy of the far-triazine−NO_3^- fragment (see Table 3), the basis is further augmented with two diffuse s and p functions with exponents 0.0138 and 0.0108 for carbon, 0.0167 and 0.0144 for nitrogen, and 0.0206 and 0.0171 for oxygen.[45] The use of these additional diffuse functions allows a stable QMC simulation in this compound where the triazine and NO_3^- molecules are at very large distances (about 7 Å). Further augmentation of the basis with two diffuse *d* functions for all heavier atoms does not change the binding energy of the compound.

The parameters in the Jastrow factor are always optimized within VMC by energy minimization[46] and, when stated, the coefficients of the orbital expansions over the atomic Gaussian basis are simultaneously optimized with the Jastrow component. Otherwise, orbitals from a B3LYP density functional theory[36,47] calculation are employed, which are obtained using the same pseudopotentials and basis set with the program GAMESS-(US).[48] An imaginary time step of 0.075 a.u. is used in the DMC calculations.

As side test, we compute the DMC binding energy and equilibrium distance of the prototypical triazine−chloride complex with the ion along the C_3 axes of the ring, which has been the subject of several MP2 studies.[2,6,7,10,9,13] We perform a correlated sampling run[49] using as reference the MP2/aug-cc-pVDZ geometry with a chloride-centroid distance of 3.13 Å,[7] and the corresponding fully optimized QMC wave function. We find a DMC equilibrium distance of 3.24 Å, which is in

TABLE 1: DFT/BLYP-DCACP and DMC Binding Energies in kcal/mol of the Triazine−NO_3^- Complex[a]

geometry	R_0	R'_0	DFT	DMC	MP2
DFT parallel	3.18		−6.7	−5.1(3)	
MP2 parallel	2.90[b]			−4.9(3)[d]	−6.8[b]
DFT T-like	3.69	3.07	−8.8	−6.7(3)	
MP2 T-like		2.75[c]			−8.4[c]

[a] The parallel and T-like geometries corresponding to the MP2 and DFT/BLYP-DCACP equilibrium distances are shown. The MP2 binding energies are also given when available. R_0 and R'_0 are the equilibrium distances in Å between the ring centroid and the nitrogen atom of NO_3^-, and between the centroid and the closest oxygen atom of NO_3^-, respectively. The statistical error on the last figure of the DMC binding energy is given in parentheses. [b] Reference 7. MP2/aug-cc-pVDZ. [c] Reference 24. MP2/6-311++G(3df,p). [d] Wave function fully optimized with VMC.[50]

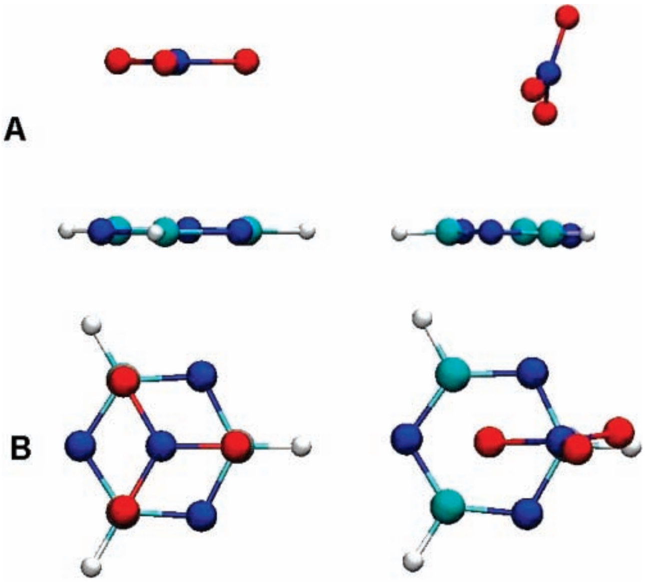

Figure 1. Side (A) and top (B) view of the triazine−nitrate complex in the parallel geometry (left) and in the T-like form (right).

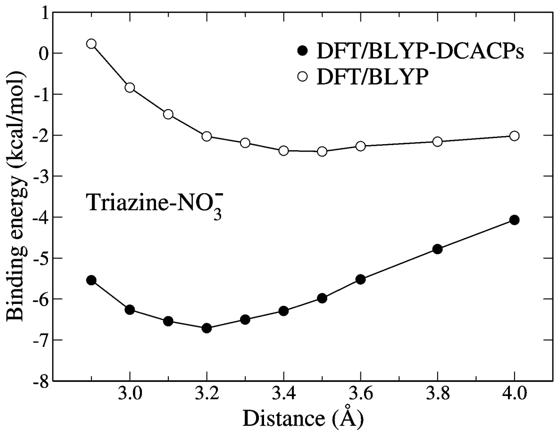

Figure 2. Binding energy of the triazine−NO_3^- system in the parallel geometry as a function of the distance between the centroid of the triazine ring and the nitrogen atom of NO_3^-. The curves are computed within DFT/BLYP with and without the DCACPs.

the range of the MP2 values obtained with different basis sets.[7] The DMC binding energy of 6.0(3) kcal/mol is slightly smaller than the MP2/aug-cc-pVDZ value of 6.93 kcal/mol.[7] We note that using optimized or B3LYP orbitals in the determinantal component of the wave functions yields statistically equivalent results even though the B3LYP approach underestimates the binding energy by about 2 kcal/mol.[9]

3. Results

To investigate cooperative effects of anion−π and π−π interactions in the unusual triazine−triazine−nitrate complex observed experimentally, we first need to characterize how the anion−π and π−π fragments are separately stabilized. Studying these smaller components also allows us to access the performance of QMC and in particular of the semiempirical DCACP approach, by comparing to MP2 or CCSD(T) calculations when available.

3.1. Triazine and NO_3^-. The triazine−NO_3^- complex represents one of the first examples of anion−π interactions observed experimentally[23,24] and has already been the subject of several computational studies both at the DFT and at the MP2 level.[7,23,24] Thus, it is an ideal system to assess the accuracy and transferability of the DCACPs in describing this novel weak interactions as all the atomic elements in the complex are available in the current library of dispersion corrected pseudopotentials.[35]

In Table 1, we show the binding energy and the equilibrium distance between the ring centroid and the nitrogen of NO_3^-, calculated with different approaches. We focus first on the symmetrical geometry where the plane of the nitrate is parallel to the triazine plane with the nitrogen of the anion located on top of the ring centroid and the oxygens facing the carbon atoms (Figure 1). We find that DFT/BLYP-DCACP gives a binding energy that is very close to the one obtained within the MP2 approach[7] but with a slightly larger (about 10%) equilibrium distance. DMC gives a binding energy ≈1.7 kcal/mol smaller than the DFT and MP2 values. A DMC equilibrium distance of about 2.9 Å is estimated in a correlated sampling run using as reference geometry the MP2 geometry and the corresponding fully optimized QMC wave function.[49] In Figure 2, we show the DFT binding energies obtained with the standard BLYP and the BLYP-DCACP pseudopotentials for the parallel geometry at different distances between the planes. The structure of the fragments is kept fixed at the optimal geometry of the complex while changing the triazine−nitrate distance. The computed BLYP binding energy of 2.4 kcal/mol is in line with the value previously obtained with a Slater-type orbital ET-pVQZ basis.[23] It clearly appears that the dispersion corrections have a very large effect on the description of the anion−π interactions. With the inclusion of the DCACP pseudopotentials, the binding energy increases from 2.4 to 6.7 kcal/mol and the equilibrium distance decreases by about 6%.

The triazine−nitrate complexes observed experimentally[23,24] show, however, a very different structure from the more intuitive face-to-face configuration. This observation prompted further calculations both at the DFT and at the MP2 level,[23,24] which yield an energetically lower T-like arrangement of the triazine−nitrate complex. As shown in Table 1, the structure and the binding energy of the T-like complex computed within DFT/BLYP-DCACP compare well with the MP2 values.[24] In particular, the dispersion corrected potentials predict this configuration to be more stable than the parallel arrangement by about 2 kcal/mol. Similarly to the MP2 results, we find that the two oxygens of the nitrate point toward the triazine plane, one facing the ring centroid and the other facing one hydrogen atom at a distance $d_{O\cdots H} = 2.52$ Å (see also Figure 1). The interaction with the hydrogen appears to further stabilize this geometrical arrangement. The shortest oxygen-centroid distance R'_0 predicted by DFT/BLYP-DCACP is again about 10% larger than the MP2 value. The DMC calculations performed using the DFT optimized complexes give the same trend for the binding energy

TABLE 2: DFT/BLYP-DCACP and DMC Binding Energies in kcal/mol of Different Conformations of the Triazine−Triazine Dimer[a]

geometry		R_0	DFT	DMC	MP2	CCSD(T)
DFT	0°	3.80	−1.7	−0.6(3)		
DFT	30°	3.70	−2.5	−1.6(3)		
DFT	60°	3.60	−3.5	−2.2(3)		
MP2[b]	60°	3.40	−	−2.8(3)	−3.8[b]	−2.8[b]
DFT	30° bent	3.79	−2.9	−2.1(3)		
DFT	60° bent	3.61	−3.4			

[a] The equilibrium distance R_0 in Å is between the centroids of the two rings and the angle indicates their relative rotation. [b] References 51 and 52 with a diffuse cc-pVDZ′ basis set.

with the T-like geometry being the most stable. DMC results, however, indicate that both DFT and MP2 tend to overestimate the binding energy by ≈2 kcal/mol.

3.2. Triazine Dimer. The DCACPs have been developed with the main aim of improving the generally poor description of $\pi-\pi$ interactions within DFT. The triazine dimer makes no exception in this respect, with the BLYP functional giving an unbound state. At the contrary, ab initio correlated methods such as MP2 and CCSD(T) find a bound state with the optimal conformation being a stacked complex with a 60° relative orientation and a vertical distance of 3.4 Å.[51,52] As shown in Table 2, the MP2 method tends to overestimates the binding energy in comparison with the more accurate CCSD(T) approach, a feature that appears to be general in the MP2 description of van der Waals complexes.[51−53]

In Table 2, we show the results for the triazine dimer obtained with the DFT/BLYP-DCACP approach. We consider the face-to-face conformation with relative orientations, 0°, 30°, and 60°, between the two triazine molecules (Figure 3). All structures are bound with the binding energy increasing as we move from 0° to 60°. The DFT-DCACP global minimum at 60° is consistent with the MP2 finding but has a slightly smaller binding energy and a centroid-to-centroid distance 6% larger. DMC calculations performed on the DFT optimized geometries display the same trend as DFT but give a systematically smaller binding energy by about 1 kcal/mol. We note that, at the MP2 geometry, the DMC binding energy is equal to the CCSD(T) prediction. Once more, these results indicate that the BLYP-DCACPs are able to predict the proper trend and global minimum of the weakly bound triazine dimer although they slightly overestimate the binding energy similarly to the MP2 approach.

In the crystalline structure[23] containing the triazine−triazine−nitrate complex, an unusual triazine−triazine moiety is observed: The planes of the triazine molecules are slightly off-centered with a centroid-to-centroid distance of 3.45 Å and have a relative orientation of about 30° with a dihedral angle of about 15°. If we optimize the triazine dimer within DFT-BLYP-DCACP starting from this experimental conformation, we find a local minimum very similar to the experiment, that is, a distance between the centroids of 3.79 Å and a dihedral angle between the two rings of 11° (see Figure 3). As shown in Table 2, the predicted binding energy for this local minimum is only 0.6 kcal/mol lower than the global minimum. However, the bending slightly stabilizes the dimer with respect to the parallel conformation at the same angle of 30°. For the bent conformation, DMC gives the same energy within statistical error as for the DFT global minimum geometry.

3.3. Cooperativity of Anion−π−π Interactions. We now focus on the experimental triazine−triazine−nitrate complex observed in ref 23 to understand the unusual structural features and quantify the stabilization induced on the anion−π system by $\pi-\pi$ stacking. The relevant anion−π−π unit of the crystalline structure represents the starting point for our calculations and is shown in Figure 4 together with the DFT/BLYP-DCACP optimal geometry. The similarity between the experimental and theoretical complexes is remarkable: The two triazine are staggered by about 30° and bent and slip with respect to each other with the nitrate bound in a T-like configuration. Moreover, the nitrogen of the anion is displaced with respect to the normal through the centroid of the ring, consistently with the experiment. More specifically, we find a centroid-to-centroid distance of 3.74 Å and a distance from the centroid to the N of NO_3^- of 3.50 Å as compared to the experimental values of 3.45 and 3.71 Å, respectively. The two aromatic rings form a dihedral angle of 22°, close to the experimental value of 18°. Finally, two oxygen atoms of the nitrate are interacting with the triazine ring, similarly to the observed structure. A more detailed comparison with the experimental structure is not appropriate as the experimental complex is embedded in the crystalline environment, which may induce further distortions. We note that, with respect to the geometries of the subunits separately optimized, the presence of the nitrate does not significantly change the centroid−centroid distance but yields a larger tilt angle between the rings. As for triazine−nitrate system, the main geometrical effect is that the nitrate is more parallel and closer to the ring with a centroid-oxygen distance of 2.98 Å.

The total computed binding energy of this anion−π−π complex is −12.4 kcal/mol. To establish the stabilization effect induced by $\pi-\pi$ stacking on this supramolecular complex, we separately compute the $\pi-\pi$ and anion−π contributions to the binding energy. We extract from the optimized structure the three fragments corresponding to the triazine dimer and the two possible triazine−nitrate units and compute their binding energies, which are listed in Table 3. By subtracting these contributions from the total binding energy of the anion−π−π system, we derive a cooperative contribution to the binding energy of 0.8 kcal/mol, which corresponds to a stabilization enhancement of about 6%. The cooperative energy predicted by DMC using the DFT geometries is compatible with the DFT value within two standard deviations, and the DMC binding energies of the individual fragments are always lower, as already pointed out in the previous sections. In particular, the compound given by the nitrate and the distant triazine ring is unbound within DMC due to geometrical deformations of the molecules within the triazine−triazine−nitrate complex.

We note that the triazine rings are not in the optimal staggered configuration of 60° (see Table 2) but have a relative orientation of about 30°. This is certainly due to the geometrical constraints within the crystalline framework as the triazine rings are strongly coordinated via a complex network to the metal centers of the compound. To generate a triazine−triazine−nitrate complex arrangement consistent with the optimal geometries for the separate fragments, we thus start from a structure in which the triazine rings are parallel in the optimal 60° orientation, with the nitrate in the T-like form and two oxygens interacting with the ring (Figure 5). The geometry optimization shows that the relative orientation remains at 60°, and the centroid−centroid distance is unchanged with respect to the isolated dimer. However, the presence of the anion induces a tilt of about 14° of the triazine close to it, which is likely induced by the interaction between one oxygen of the nitrate and one hydrogen of the ring. As expected, the binding energy of this complex is slightly larger than in the structure derived

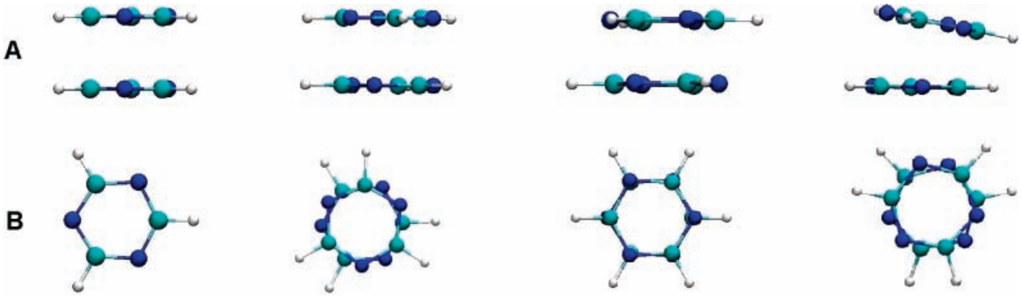

Figure 3. Side (A) and top (B) view of four different conformations of the triazine−triazine dimer. From left to right, the two molecules are rotated with respect to each other by 0°, 30°, and 60°. The bent geometry (right) is rotated by roughly 30°.

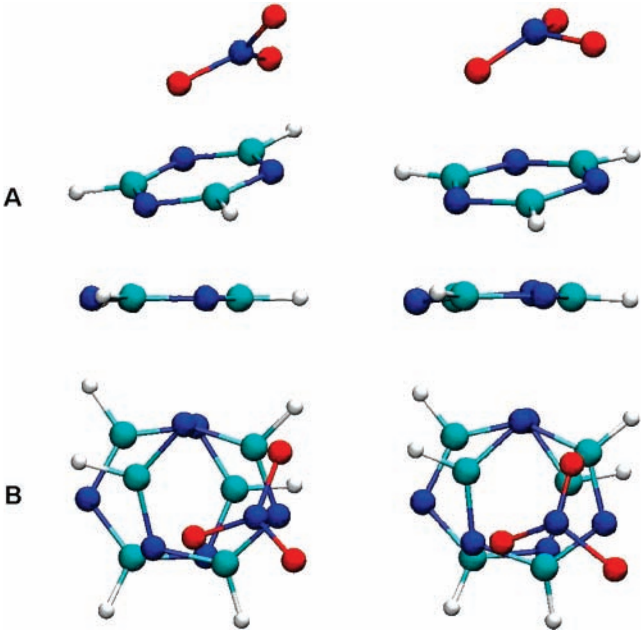

Figure 4. Side (A) and top (B) view of the triazine−triazine−NO_3^- complex as obtained within DFT/BLYP-DCACP (left) and experimentally[23] (right). In the top view, the bottom ring is parallel to the page.

TABLE 3: DFT/BLYP-DCACP and DMC Binding Energies in kcal/mol of Five π−π Complexes Interacting with NO_3^-, *i.e.*, Two Triazine (TAZ) Rings at 30°, Two TAZ Rings at 60°, Two Trifluorotriazine (TFT) at 60°, and the Two Mixed Systems with One TAZ and One TFT Ring at 60° [a]

compound	TAZ 30° DFT	TAZ 30° DMC	TAZ 60° DFT	TFT DFT	TAZ-TFT DFT	TFT-TAZ DFT
ring−ring-NO_3^-	−12.4	−8.5(2)	−13.5	−21.5	−20.3	−17.3
ring−ring	−2.8	−1.7(2)	−3.0	−0.2	−1.6	−2.6
close-ring-NO_3^-	−8.3	−6.0(2)	−8.8	−16.5	−16.5	−8.3
far-ring-NO_3^-	−0.5	0.7(2)	−0.7	−4.3	−0.7	−4.6
cooperativity	−0.8	−1.6(4)	−0.9	−0.6	−1.5	−1.8

[a] The mixed systems denoted TAZ-TFT and the TFT-TAZ have the TFT and TAZ ring closer to the NO_3^-, respectively. The geometry of the ternary compound (ring−ring-NO_3^-) is optimized within DFT/BLYP-DCACP and the geometries of the ring−ring, close-ring-NO_3^-, and far-ring-NO_3^- fragments are here kept fixed when computing their binding energies. The binding energies are obtained as the difference between the total energy and the energies of the isolated ring and NO_3^- optimized separately. For example, the binding energy of the ternary compound is given by $E_b(\text{ring−ring-}NO_3^-) = E(\text{ring−ring-}NO_3^-) - 2E(\text{ring}) - E(NO_3^-)$. The cooperative energy is defined as $E_b(\text{ring−ring-}NO_3^-) - E_b(\text{close-ring-}NO_3^-) - E_b(\text{far-ring-}NO_3^-) - E_b(\text{ring−ring})$.

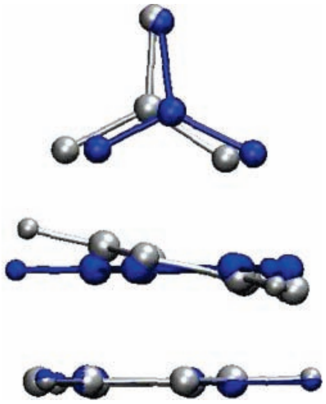

Figure 5. Triazine−triazine−NO_3^- complex with relative orientation of the rings of 60° optimized within DFT/BLYP-DCACP (gray). In blue, we show the starting symmetrical geometry.

from the experiment (see Table 3) and the cooperative effect is of comparable magnitude.

Finally, we check the effect of enhancing the π-anion interaction by substituting the hydrogens in the triazine rings at 60° with the strongly electronegative fluorine.[2,6,10] With this procedure, we generate three complexes, *i.e.*, (1) two trifluorotriazine rings with a nitrate, (2) one triazine and one trifluorotriazine coordinated with the nitrate, and (3) one trifluorotriazine and one triazine coordinated with the nitrate. As seen in Table 3, the total binding is increased by the fluorine substitution due to the stronger attractive interaction between the nitrate and the trifluorotriazine ring(s). However, this increase does not always correlate with a cooperative enhancement of the π-anion interaction by π−π stacking. In particular, in the complex with two trifluorotriazine rings, the cooperative effect is smaller than in the original system with two triazine rings as the π−π system is now very weakly bound: The binding energy of the ring−ring fragment is only 0.2 kcal/mol, significantly reduced from the 2.0 kcal/mol of the trifluorotriazine dimer optimized in the absence of the nitrate. This small binding can be explained with the strong deformation of the trifluorotriazine ring close to the nitrate, with one of the fluorine's bending out of the ring plane away from one of the nitrate oxygens.

In the mixed triazine−trifluorotriazine compounds, we observe instead a more favorable balance of π−π and anion−π interactions, leading to an increased cooperativity. In both complexes, the ring−ring fragment is still significantly bound even though its binding energy is smaller than the optimal value of 3.2 kcal/mol for the isolated dimer. The ring−ring binding energy of the complex with the triazine coordinated to the nitrate is larger by about 1 kcal/mol than the energy obtained in the case of the trifluorotriazine coordinated to the nitrate. The reduced binding of the latter is due to a strong deformation of the trifluorotriazine ring vicinal to the nitrate, similarly to what observed in the compound with two trifluorotriazine rings. Correspondingly, the largest cooperative effect is observed in the mixed complex with the triazine coordinated to the nitrate where the non-additive contribution amounts to roughly 10% of the total binding energy. Finally, we note that the cooperative effect is always present in all the studied complexes, though this does not appear to be a general feature[18] of anion−π−π complexes, and points to the very versatile nature of the triazine moiety in supramolecular chemistry.[54]

4. Conclusions

Using state-of-the-art dispersion corrected DFT and QMC calculations, we have investigated the geometrical and energetic effects induced by π−π stacking on the anion−π system of the unusual triazine−triazine−nitrate complex recently observed experimentally. We have reproduced and rationalized the highly asymmetrical features of the structure, which are not imposed by the coordination of the anion−π−π subunit within the particular synthesized compound. We show that the two triazines are staggered and bent and slip with respect to each other with the nitrate bound off-center in a T-like configuration. The stabilization induced by π−π stacking amounts energetically to about 6% of the total binding energy. An increased cooperative effect of 10% is obtained if the hydrogens in one of the triazine rings are substituted with the strongly electronegative fluorine atoms and the dimer is further staggered in a 60° orientation. We want to emphasize that the theoretical investigation of a realistic anion−π−π system as the one treated in this paper is particularly demanding, as correlation plays an important role; moreover, the system is not small and must be treated without symmetry constraints. We find that the use of the recently proposed dispersion corrected DFT approach represents a good compromise between accuracy and the ability to study complex and realistic systems involving weak interactions.

Acknowledgment. We thank P. Gamez and J. Reedijk for useful discussions. M.Z. is supported by the Stichting voor Fundamenteel Onderzoek der Materie (FOM). We acknowledge the support from the Stichting Nationale Computerfaciliteiten (NCF-NWO) for the use of the SARA supercomputer facilities.

Supporting Information Available: Optimized geometries and total energies. This material is available free of charge via the Internet at http://pubs.acs.org.

References and Notes

(1) Beer, P. D.; Gale, P. A. *Angew. Chem., Int. Ed.* **2001**, *40*, 486.

(2) Mascal, M.; Armstrong, A.; Bartberger, M. B. *J. Am. Chem. Soc.* **2002**, *124*, 6274.

(3) Akkorta, I.; Rozas, I.; Elguero, J. *J. Am. Chem. Soc.* **2002**, *124*, 8593.

(4) Quiñonero, D.; Garau, C.; Frontera, A.; Ballester, P.; Costa, A.; Deya, P. M. *Chem. Phys. Lett.* **2002**, *359*, 486.

(5) Garau, C.; Quiñonero, D.; Frontera, A.; Costa, A.; Ballester, P.; Deya, P. M. *Chem. Phys. Lett.* **2003**, *370*, 7.

(6) Garau, C.; Quiñonero, D.; Frontera, A.; Ballester, P.; Costa, A.; Deya, P. M. *Chem. Phys. Chem* **2003**, *4*, 1344.

(7) Kim, D.; Tarakeshwar, P.; Kim, K. S. *J. Phys. Chem. A* **2004**, *108*, 1250.

(8) Garau, C.; Frontera, A.; Quiñonero, D.; Ballester, P.; Costa, A.; Deya, P. M. *J. Phys. Chem. A* **2004**, *108*, 9423.

(9) Quiñonero, D.; Garau, C.; Frontera, A.; Ballester, P.; Costa, A.; Deya, P. M. *J. Phys. Chem. A* **2005**, *109*, 4632.

(10) Garau, C.; Quiñonero, D.; Frontera, A.; Ballester, P.; Costa, A.; Deya, P. M. *J. Phys. Chem. A* **2005**, *109*, 9341.

(11) Garau, C.; Frontera, A.; Ballester, P.; Quiñonero, D.; Costa, A.; Deya, P. M. *Eur. J. Org. Chem* **2005**, 179.

(12) Frontera, A.; Saczewski, F.; Gdaniec, M.; Dziemidowicz-Borys, E.; Kurland, A.; Deya, P. M.; Quiñonero, D.; Garau, C. *Chem. Eur. J.* **2005**, *11*, 6590.

(13) Mascal, M. *Angew. Chem., Int. Ed.* **2006**, *45*, 2890.

(14) Clements, A.; Lewis, M. *J. Phys. Chem. A* **2006**, *110*, 12705.

(15) Quiñonero, D.; Frontera, A.; Garau, C.; Ballester, P.; Costa, A.; Deya, P. M. *Chem. Phys. Chem* **2006**, *7*, 2487.

(16) Berryman, O. B.; Bryantsev, V. S.; Stay, D. P.; Johnson, D. W.; Hay, B. P. *J. Am. Chem. Soc.* **2007**, *129*, 48.

(17) Quiñonero, D.; Frontera, A.; Escusero, D.; Ballester, P.; Costa, A.; Deya, P. M. *Chem. Phys. Chem* **2007**, *8*, 1182.

(18) Frontera, A.; Quiñonero, D.; Costa, A.; Deya, P. M. *New J. Chem.* **2007**, *31*, 556.

(19) Rosokha, Y. S.; Lindeman, S. V.; Rosokha, S. V.; Kochi, J. K. *Angew. Chem., Int. Ed.* **2004**, *43*, 4650.

(20) Demishko, S.; Dechert, S.; Meyer, F. *J. Am. Chem. Soc.* **2004**, *126*, 4508.

(21) De Hoog, P.; Gamez, P.; Mutikainen, I.; Turpeinen, U.; Reedijk, J. *Angew. Chem., Int. Ed.* **2004**, *43*, 5815.

(22) Schottel, B. L.; Chifotides, H. T.; Shatruk, M.; Chouai, A.; Pérez, L. M.; Bacsa, J.; Dunbar, K. R. *J. Am. Chem. Soc.* **2006**, *128*, 5859.

(23) Casellas, H.; Massera, C.; Buda, F.; Gamez, P.; Reedijk, J. *New J. Chem.* **2006**, *30*, 1561.

(24) Maheswari, P. U.; Modec, B.; Pevec, A.; Kozlevcar, B.; Massera, C.; Gamez, P.; Reedijk, J. *Inorg. Chem* **2006**, *45*, 6637.

(25) Gamez, P.; Mooibroek, T. J.; Teat, S. J.; Reedijk, J. *Acc. Chem. Res.* **2007**, *40*, 435.

(26) Lakshminarayanan, P. S.; Ravikumar, I.; Suresh, E.; Ghosh, P. *Inorg. Chem.* **2007**, *46*, 4769.

(27) Casellas, H.; Roubeau, O.; Teat, S. J.; Mascocchi, N.; Galli, S.; Sironi, A.; Gamez, P.; Reedijk, J. *Inorg. Chem.* **2007**, *46*, 4583.

(28) Hettche, F.; Hoffman, R. W. *New J. Chem.* **2003**, *27*, 172.

(29) Berryman, O. B.; Hof, F.; Hynes, M. J.; Johnson, D. W. *Chem. Commun.* **2006**, 506.

(30) Akkorta, I.; Rozas, I.; Elguero, J. *J. Org. Chem.* **1997**, *62*, 4687.

(31) von Lilienfeld, O. A.; Tavernelli, I.; Rothlisberger, U.; Sebastiani, D. *Phys. Rev. Lett.* **2004**, *93*, 153004.

(32) von Lilienfeld, O. A.; Tavernelli, I.; Rothlisberger, U.; Sebastiani, D. *Phys. Rev. B* **2005**, *71*, 195119.

(33) von Lilienfeld, O. A.; Andrienko, D. *J. Chem. Phys* **2006**, *124*, 054307.

(34) Tkatchenko, A.; von Lilienfeld, O. A. *Phys. Rev. B* **2006**, *73*, 153406.

(35) Lin, I-C.; Coutinho-Neto, M. D.; Felsenheimer, C.; von Lilienfeld, O. A.; Tavernelli, I.; Rothlisberger, U. *Phys. Rev. B* **2007**, *75*, 205131.

(36) Becke, A. D. *Phys. Rev. A* **1988**, *38*, 3098. Lee, C. T.; Yang, W. T.; Parr, R. G. *Phys. Rev. B* **1988**, *37*, 785.

(37) Troullier, N.; Martins, J. L. *Phys. Rev. B* **1991**, *43*, 1993.

(38) Hutter, J. M.; *et al.* CPMD, Version 3.11.1, Copyright IBM Corp. 1990−2006, copyright MPI-FKF Stuttgart 1997−2004; http://www.cpmd.org.

(39) Hockney, R. W. *Methods Comput. Phys.* **1970**, *9*, 136.

(40) Foulkes, W. M. C.; Mitas, L.; Needs, R. J.; Rajagopal, G. *Rev. Mod. Phys.* **2001**, *73*, 33.

(41) Hammond, B. L.; Lester, W. A., Jr.; Reynolds, P. J. *Monte Carlo Methods in Ab Initio Quantum Chemistry*; World Scientific: Singapore 1994.

(42) Filippi, C.; Umrigar, C. J. *J. Chem. Phys.* **1996**, *105*, 213. The Jastrow factor is adapted to deal with pseudo-atoms and the scaling factor κ is set to 0.5 for all atoms.

(43) CHAMP is a quantum Monte Carlo program package written by C. J. Umrigar and C. Filippi and collaborators; http://www.ilorentz.org/filippi/champ.html.

(44) Burkatzki, M.; Filippi, C.; Dolg, M. *J. Chem. Phys.* **2007**, *126*, 234105. http://www.tc.uni-koeln.de/data/psdb/intro.html.

(45) The exponents of the diffuse functions are taken from the aug-cc-pVDZ basis sets, http://www.emsl.pnl.gov/forms/basisform.html.

(46) Umrigar, C. J.; Toulouse, J.; Filippi, C.; Sorella, S.; Henning, R. *Phys. Rev. Lett.* **2007**, *98*, 110201.

(47) Becke, A. D. *J. Chem. Phys.* **1993**, *98*, 5648.

(48) Schmidt, M. W.; Baldridge, K. K.; Boatz, J. A.; Elbert, S. T.; Gordon, M. S.; Jensen, J. H.; Koseki, S.; Matsunaga, N.; Nguyen, K. A.; Su, S. J.; Windus, T. L.; Dupuis, M.; Montgomery, J. A. *J. Comput. Chem.* **1993**, *14*, 1347.

(49) Filippi, C.; Umrigar, C. J. *Phys. Rev. B* **2000**, *61*, R16291.

(50) The wave function is fully optimized in VMC within energy minimization. The use of B3LYP orbitals yields a statistically compatible binding energy of 4.4(3) kcal/mol.

(51) Hobza, P. *Annu. Rep. Prog. Chem. Sect. C* **1996**, *93*, 257.

(52) Sponer, J.; Hobza, P. *Chem. Phys. Lett.* **1997**, *267*, 263.

(53) Sorella, S.; Casula, M.; Rocca, D. *J. Chem. Phys.* **2007**, *127*, 014105.

(54) Gamez, P.; Reedijk, J. *Eur. J. Inorg. Chem.* **2006**, 29.